

# Comparisons of topological properties in autism for the brain network construction methods

Min-Hee Lee<sup>a\*</sup>, Dong Youn Kim<sup>a</sup>, Sang Hyeon Lee<sup>a</sup>, Jin Uk Kim<sup>a</sup>, Moo K. Chung<sup>b</sup>  
<sup>a</sup>Department of Biomedical Engineering, Yonsei University, Wonju, Korea; <sup>b</sup>Waisman Laboratory for Brain Imaging and Behavior, University of Wisconsin, Madison, WI, USA

## ABSTRACT

Structural brain networks can be constructed from the white matter fiber tractography of diffusion tensor imaging (DTI), and the structural characteristics of the brain can be analyzed from its networks. When brain networks are constructed by the parcellation method, their network structures change according to the parcellation scale selection and arbitrary thresholding. To overcome these issues, we modified the  $\epsilon$ -neighbor construction method proposed by Chung et al. (2011). The purpose of this study was to construct brain networks for 14 control subjects and 16 subjects with autism using both the parcellation and the  $\epsilon$ -neighbor construction method and to compare their topological properties between two methods. As the number of nodes increased, connectedness decreased in the parcellation method. However in the  $\epsilon$ -neighbor construction method, connectedness remained at a high level even with the rising number of nodes. In addition, statistical analysis for the parcellation method showed significant difference only in the path length. However, statistical analysis for the  $\epsilon$ -neighbor construction method showed significant difference with the path length, the degree and the density.

**Keywords:** Diffusion tensor imaging (DTI), Tractography, Topological Properties, Brain Network, Autism,  $\epsilon$ -neighbor construction method, Parcellation

## 1. INTRODUCTION

Diffusion tensor imaging (DTI) which measures the diffusion of water molecules is sensitive to microstructure of brain tissue. Structural brain networks can be constructed from the white matter fiber tractography based on DTI, and the structural characteristics of the brain can be analyzed from its networks. Recently, attempts to model the human brain as a network of brain regions connected by anatomical tracts or functional associations have attracted considerable interest, since characterizing this structural and functional connectivity could impact studies of brain pathology and developmental disorders<sup>1</sup>. Comparisons of structural or functional network topological properties between subjects could reveal putative connectivity abnormalities in neurological and psychiatric disorders<sup>2</sup>.

Many researchers have constructed brain networks using the parcellation method in white matter fiber tractography. This method is somewhat problematic in that network structure is influenced by changes in both the parcellation scale and the thresholding connectivity matrix. To overcome these problems, Chung et al. proposed a network graph modeling technique that does not involve a parcellation, called the  $\epsilon$ -neighbor construction technique<sup>3</sup>. This method considers only two endpoints of each tract, designated as nodes on the graph, while tracts are designated as edges. In this study, we propose a modified version of the  $\epsilon$ -neighbor construction method. We constructed brain networks for 14 control subjects and 16 subjects with autism using both the parcellation and the  $\epsilon$ -neighbor construction method and then compared their topological properties including path length, degree, density between control and autism subjects.

## 2. METHODS

### 2.1 Data acquisition and pre-processing

We analyzed DTI data from a total of 30 subjects, matched for age, handedness, IQ, and head size. Diffusion-weighted images were obtained not only for a single ( $b = 0$ ) reference image, but also for 12 non-collinear diffusion-encoding directions, with a diffusion weighting factor of  $b = 1000$  s/mm<sup>2</sup>. Distortion associated with eddy currents and head motion for each dataset was adjusted using automated image registration (AIR)<sup>4</sup>. Distortions from field inhomogeneities

---

\* Min-Hee Lee. e-mail [MinHLee@yonsei.ac.kr](mailto:MinHLee@yonsei.ac.kr); phone +82-33-760-2499

were adjusted using custom software algorithms<sup>5</sup>. The six tensor elements were calculated using non-linear fitting methods<sup>6</sup>. We have used a nonlinear tensor image registration algorithm for spatial normalization of DTI data, and performed the streamline based tractography using the TENSOR Deflection (TEND) algorithm<sup>7,8</sup>. The results of preprocessing and tractography are shown in Fig. 1.

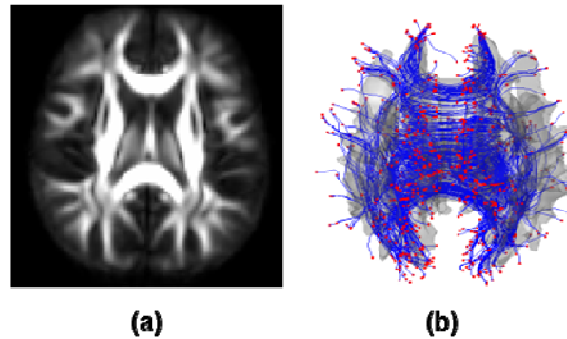


Figure 1. The results of preprocessing (a) Template FA map in the normalized space. Individual subjects are nonlinearly transformed into this space. (b) Tractography using TEND algorithm is performed in this normalized space. Tract endpoints are identified and colored red.

## 2.2 $\epsilon$ -neighbor construction method

Accepting the premise that the entire brain contains total  $i$  tracts, the  $j$ -th tract will have two endpoints,  $e_{j1}$  and  $e_{j2}$ . In our network graph construction, we only considered two endpoints. Tract endpoints were considered to be nodes; tracts were considered to be edges in our graph. The 3-D graph is described as  $G_k = \{V_k, E_k\}$ , with vertex set  $V_k$  and edge set  $E_k$  at the  $k$ -th iteration.  $d(p, G_k)$  is defined as the shortest Euclidean distance between point  $p$  of graph  $G_k$  and all points in  $V_k$ , i.e.

$$d(p, G_k) = \min_{q \in V_k} \|p - q\|. \quad (1)$$

Point  $p$  is designated as an  $\epsilon$ -neighbor of graph  $G_k$  if  $d(p, G_k) \leq \epsilon$ . Since a tract has two endpoints, the  $\epsilon$ -neighbor construction method begins with graph  $G_1$ , with  $V_1 = \{e_{11}, e_{12}\}$  and  $E_1 = \{e_{11}e_{12}\}$ . Next, the endpoints  $e_{21}$  and  $e_{22}$  from the second tract are added to the existing graph  $G_1$ . Note that the  $\epsilon$ -neighbor construction method is performed in order from the longest tract to the shortest tract to guarantee the uniqueness. Figure 2 shows six possibilities of the  $\epsilon$ -neighbor construction.

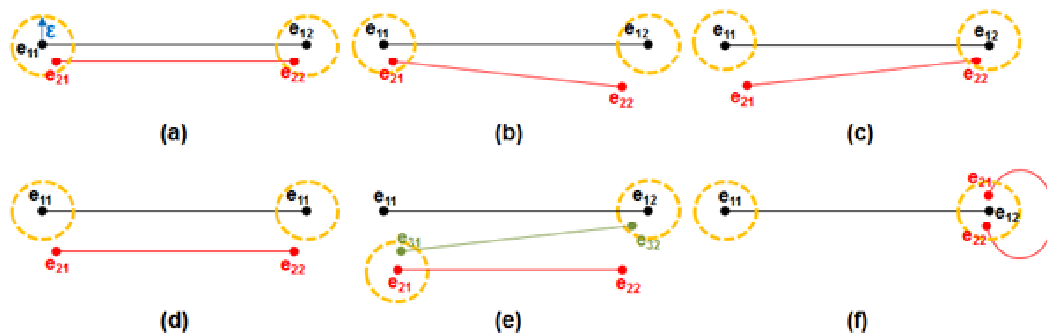


Figure 2. Six possibilities of the  $\epsilon$ -neighbor construction method : (a)  $e_{21}$  and  $e_{22}$  are all  $\epsilon$ -neighbors of  $G_1$ . (b) Only  $e_{21}$  is an  $\epsilon$ -neighbor of  $G_1$ . (c) Only  $e_{22}$  is an  $\epsilon$ -neighbor of  $G_1$ . (d) Neither  $e_{21}$  nor  $e_{22}$  is an  $\epsilon$ -neighbor of  $G_1$ . (e)  $e_{31}$  is an  $\epsilon$ -neighbor of  $e_{21}$  in  $G_2$  and  $e_{32}$  is an  $\epsilon$ -neighbor of  $e_{12}$  in  $G_2$ . (f)  $e_{21}$  and  $e_{22}$  are  $\epsilon$ -neighbors of  $e_{11}$  or  $e_{12}$  in  $G_1$ . This relationship was considered to be noise, since it results in a circular tract.

The resultant 3D graph can be parameterized by transforming the existing graph to an adjacency matrix. The adjacency matrix  $A = (adj_{ij})$  of a graph is constructed by adding new edges to the existing edge set. If nodes  $i$  and  $j$  are connected,  $adj_{ij} = 1$ . Otherwise,  $adj_{ij} = 0$ . The  $\epsilon$ -neighbor construction results are shown in Fig. 3 (a), (b).

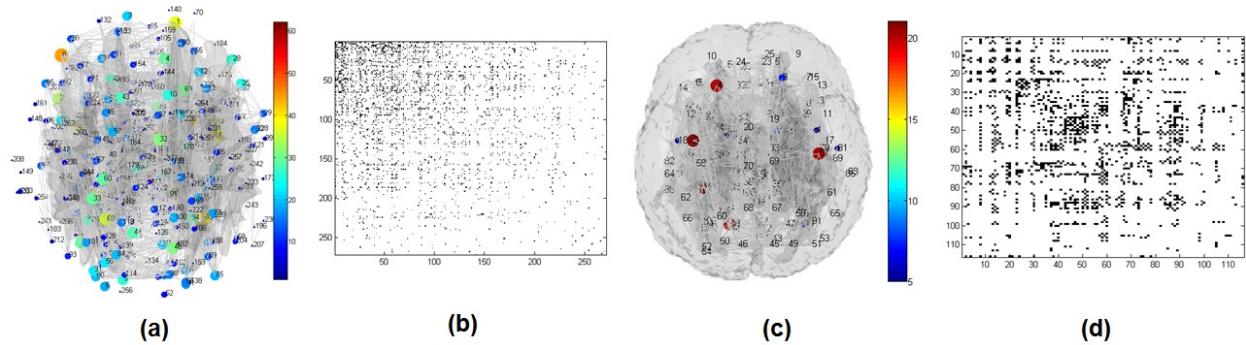


Figure 3. The results of the network construction. (a) The network with each vertex colored according to its degrees using the  $\epsilon$ -neighbor construction method. (b) An adjacency matrix for the network (a). (c) The network with each vertex colored according to its degrees using the parcellation method. (d) An adjacency matrix for the network (c).

### 2.3 Parcellation method

To construct a network graph using the parcellation method, we used the automated anatomical labeling (AAL) template. Let  $G(n) = \{x_1, x_2, \dots, x_n\}$ ,  $n = 1, 2, \dots, 116$ , denote the volume encapsulated by the  $n$ -th node composing an 116-node parcellation. Let  $S$  and  $E$  be the endpoints of each tract. An adjacency matrix  $A = (adj_{ij})$  was defined by the following equation:

$$adj_{ij} = \sum_{i \neq j} I_{\{S \in G(i)\}} I_{\{E \in G(j)\}} + I_{\{S \in G(j)\}} I_{\{E \in G(i)\}} \quad (2)$$

where if the endpoint  $S$  lies at the region  $G(i)$ ,  $I_{\{S \in G(i)\}} = 1$  otherwise  $I_{\{S \in G(i)\}} = 0$ <sup>9</sup>. As a result, we can construct adjacency matrix that defines the undirected weighted graph. In this study, however, we considered only undirected binary graph. Therefore, we binarized the weighted graph simply by assigning one to all non-zero entries for each adjacency matrix. The results of the network construction using the parcellation method are shown in Fig. 3 (c), (d).

### 2.4 Topological properties

Complex networks recently have received attention from a range of disciplines, including social science, information science, biology, and physics<sup>10</sup>. Complex network analysis is an approach that characterizes datasets and describes the properties of complex systems by quantifying the topologies of their associated networks. Complex network analysis is based on graph theory, a mathematical approach for studying networks<sup>2</sup>. In this study, we used topological properties such as path length, degree, and density to analyze the whole brain networks.

In the brain, functional integration is the ability to combine information from multiple brain regions. Measure of this integration is often based on the concept of a path. Paths represent potential routes of information flow and functional proximity between pairs of brain regions in the structural brain networks. The absence of paths between any pair of brain regions can cause no functional interactions<sup>2, 10</sup>. Undirected binary path length is equal to the number of edges in the path. The shortest path length between  $v_i$  and  $v_j$ , with  $v_i, v_j \in V$  and graph  $G = (V, E)$  with vertex set  $V$ , edge set  $E$  is  $d(v_i, v_j)$ ; the average path length or characteristic path length is defined by the following equation:

$$l_G = \frac{1}{n(n-1)} \sum_{i,j} d(v_i, v_j) \quad (3)$$

In this definition,  $n$  refers to the number of vertices in graph  $G$ . Short paths enable effective interactions or rapid transfer of information between regions which are essential for functional integration of aspects of information flow<sup>11</sup>.

The degrees in the graph are defined as the numbers of connections with other nodes or the numbers of edges. Thus, the node degree is easily calculated as the sum of the corresponding rows or columns in the adjacency matrix. The value of degree reflects importance of node in the network. The node with high degree is interacting, structurally or functionally, with many other nodes in the network<sup>2</sup>.

The network density is a measure of the number of connections compared to the maximum possible number of connections between vertices and indicates how well the network is connected<sup>12</sup>. The network density is calculated as follows:

$$D = \frac{2|E|}{|V|(|V|-1)} \quad (4)$$

where  $E$  = edge set and  $V$  = vertex set. The maximum possible number of edges is  $0.5|V|(|V|-1)$ . In this case, the maximum density is 1 and the minimum density is 0. The maximum density means that all possible connections exist. In biological networks, however, the small number of connections compared to the all possible connections occurs<sup>12</sup>. Low densities describe sparse graphs, whereas high densities describe dense graphs. However, the appropriate criteria to use for discriminating between sparse and dense graphs are ambiguous<sup>13</sup>.

## 2.5 Comparison between the parcellation and the $\epsilon$ -neighbor construction method

To compare topological properties between the parcellation and the  $\epsilon$ -neighbor construction method, we constructed two network graphs for each subject. To construct two network graphs for each subject, some image processings are needed such as template normalization, culling tracts and matching the number of nodes. First, we performed non-linear image registration between FA and AAL templates using Ezys<sup>14</sup>. In the second, a tract was considered usable if it intersected one of the parcellation in AAL template. Culling is a necessary step to eliminate spurious tracts that do not interconnect the parcellation method<sup>9</sup>. After culling tracts, we used same usable tracts in both methods. Finally, to observe how topological properties of the network change according to the number of nodes in the both methods, we parcellated additional subregions within AAL parcellations using the algorithm proposed by Zalesky<sup>9</sup> in the parcellation method and adjusted  $\epsilon$ -radius in the  $\epsilon$ -neighbor construction method. Figure 4 shows the results of additional parcellation within AAL parcellations. Then, we compared the topological properties of the network with 116, 221, 330, 456 and 561 nodes, respectively. We performed two sample t-tests, assuming equal variance for the statistical analysis. Null hypothesis for the topological properties is that there is no difference between autism and controls.

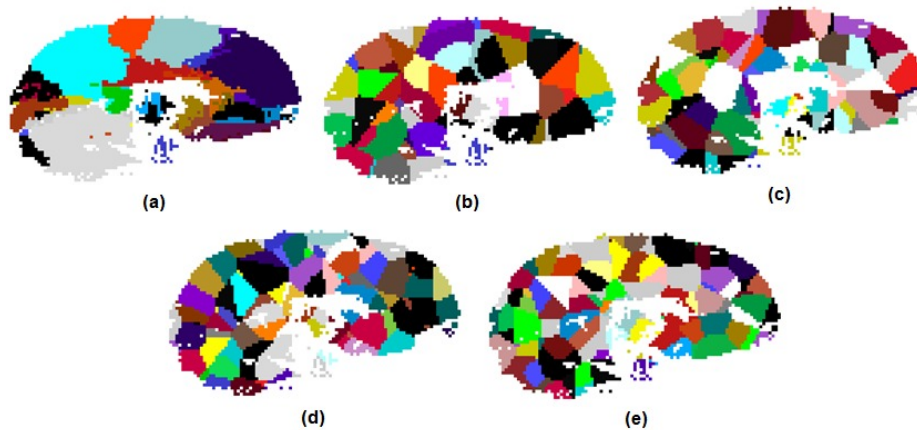


Figure 4. The results of additional parcellation. (a) 116 nodes (b) 221 nodes (c) 330 nodes (d) 456 nodes (e) 561 nodes.

## 3. RESULTS

A major problem of the parcellation method is that their network structures change according to the parcellation scale. On the other hand, our method does not change the network structures much. We analyzed the network structures in terms of connectedness, which is measured as a function of the parcellation scale and the  $\epsilon$ -radius. The results of the connectedness are summarized in Table 1.

Table 1. Connectedness comparison between the parcellation and the  $\epsilon$ -neighbor construction method

	Parcellation method		$\epsilon$ -neighbor construction method	
	Mean	SD	Mean	SD
<b>116 nodes</b>	0.9049	0.0281	1	0
<b>221 nodes</b>	0.9348	0.0233	1	0
<b>330 nodes</b>	0.8888	0.0309	0.9967	0.0036
<b>456 nodes</b>	0.8176	0.0336	0.9943	0.0043
<b>561 nodes</b>	0.7884	0.0299	0.9938	0.0040

As the number of nodes is increased, connectedness is decreased in the parcellation method. However, connectedness is almost one in the  $\epsilon$ -neighbor construction method. Therefore, we chose the parcellation scales which have less than 10% of the disconnectedness (i.e., 116 nodes and 221 nodes). Then, we compared the topological properties for the chosen two scales. The results of the comparisons of topological properties are summarized in Table 2. Statistical analysis for the parcellation method showed significant difference with the only path length. However, statistical analysis for the  $\epsilon$ -neighbor construction method showed significant difference with the path length, the degree and the density.

Table 2. Comparison of topological properties between control and autism subjects for the parcellation and the  $\epsilon$ -neighbor construction method.

		Parcellation method					$\epsilon$ -neighbor construction method				
		Control		Autism		Group comparison	Control		Autism		Group comparison
		Mean	SD	Mean	SD	Significance	Mean	SD	Mean	SD	Significance
<b>116 nodes</b>	<b>Path length</b>	2.119	0.041	2.079	0.035	0.005*	2.402	0.060	2.356	0.058	0.020*
	<b>Degree</b>	14.202	0.948	14.252	1.002	0.445	12.193	0.594	12.845	0.857	0.014*
	<b>Density</b>	0.124	0.008	0.124	0.008	0.445	0.106	0.008	0.112	0.008	0.026*
<b>221 nodes</b>	<b>Path length</b>	2.651	0.050	2.609	0.065	0.004*	2.856	0.042	2.806	0.041	0.003*
	<b>Degree</b>	11.775	0.543	12.031	0.529	0.117	10.431	0.252	10.768	0.652	0.053
	<b>Density</b>	0.054	0.003	0.055	0.002	0.117	0.046	0.002	0.049	0.004	0.019*

\*Significant at the 0.05 level

#### 4. CONCLUSIONS

The parcellation method is used in many brain network studies<sup>9</sup>. However, this method is somewhat problematic in that network structures are influenced by changes in both the parcellation scale and the thresholding connectivity matrix. To overcome these problems, we proposed the novel brain network construction method. We first compared connectedness between the parcellation and our proposed method.

In the parcellation method, when the parcellation scale becomes finer, the volume of parcellation is reduced. Thus, the probability of tracts intersecting each parcellation is decreased and a parcellation that is not intersected by any tracts is increased<sup>9</sup>. Because some nodes remain disconnected from largest connected component, connectedness is decreased in the parcellation method when the parcellation scale becomes finer. The clustering coefficient and path length of disconnected nodes from largest connected component generally were set as zero and infinity respectively, and these nodes were excluded while computing average clustering coefficient and path length to avoid computational interference. Due to the increase of the disconnected nodes, topological properties such as clustering coefficient, average path length, and small-worldness do not meaningfully characterize network structures<sup>15</sup>.

However, in our proposed method connectedness is not changed by the change of scale ( $\epsilon$ -radius). Thus, for any  $\epsilon$ -radius, we can meaningfully characterize network structures. To compare the parcellation method with our proposed method, we used the topological properties for the chosen two scales. As shown in Table 2, our results demonstrated that the statistical significance of our proposed method is better than those of the conventional parcellation method.

## ACKNOWLEDGEMENTS

This research was supported by the Leading Foreign Research Institute Recruitment Program through the National Research Foundation of Korea (NRF) funded by the Ministry of Science, ICT & Future Planning (2010-00757). The research was also supported by the Vilas Associate Award and NIH grant UL1TR000427 from the Univ. of Wisconsin. We thank Nagesh Adluru and Richard J. Davidson of University of Wisconsin-Madison for providing the data set.

## REFERENCES

- [1] Just, M. A., Cherkassky, V. L., Keller, T. A., Kana, R. K. and Minshew, N. J., "Functional and anatomical cortical underconnectivity in autism : Evidence from an fMRI study of an executive function task and corpus callosum morphometry," *Cerebral Cortex* 17 (4), 951-961(2007).
- [2] Rubinov, M. and Sporns, O., "Complex network measures of brain connectivity : uses and interpretations," *Neuroimage* 52 (3), 1059-1069 (2010).
- [3] Chung, M. K., Adluru, N., Dalton, K. M., Alexander, A. L. and Davidson, R. J. "Scalable Brain Network Construction on White Matter Fibers," *Proc. of SPIE* 7962, 79624G (2011).
- [4] Woods, R. P., Grafton, S. T., Holmes, C. J., Cherry, S. R. and Mazziotta, J. C., "Automated image registration: I. General methods and intrasubject, intramodality validation," *Journal of computer assisted tomography* 22 (1), 139-152 (1998).
- [5] Jezzard, P. and Balaban, R. S., "Correction for geometric distortion in echo planar images from B0 field variations," *Magnetic resonance in medicine* 34 (1), 65-73 (1995).
- [6] Alexander, D. C. and Barker, G. J., "Optimal imaging parameters for fiber-orientation estimation in diffusion MRI," *Neuroimage* 27 (2), 357-367 (2005).
- [7] Lazar, M., Weinstein, D.M., Tsuruda, J.S., Hasan, K.M., Arfanakis, K., Meyerand, M.E., Rowley, H.A., Haughton, V., Field, A. and Alexander, A.L., "White matter tractography using diffusion tensor deflection," *Human Brain Mapping* 18 (4), 306-321 (2003).
- [8] Cook, P. A., Bai, Y., Nedjati-Gilani, S., Seunarine, K. K., Hall, M. G., Parker, G. J. and Alexander, D. C., "Camino: Open-source diffusion-MRI reconstruction and processing," In 14th Scientific Meeting of the International Society for Magnetic Resonance in Medicine, 2759 (2006).
- [9] Zalesky, A., Fornito, A., Harding, I. H., Cocchi, L., Yücel, M., Pantelis, C. and Bullmore, E. T., "Whole-brain anatomical networks: does the choice of nodes matter?," *Neuroimage* 53 (4), 1197-1207 (2010).
- [10] Sporns, O., Chialvo, D. R., Kaiser, M. and Hilgetag, C. C., "Organization, development and function of complex brain networks," *Trends in Cognitive Sciences* 8 (9), 418-425 (2004).
- [11] Gong, G., He, Y., Concha, L., Lebel, C., Gross, D. W., Evans, A. C. and Beaulieu, C., "Mapping Anatomical Connectivity Patterns of Human Cerebral Cortex Using In Vivo Diffusion Tensor Imaging Tractography," *Cerebral Cortex* 19 (3), 524-536 (2009).
- [12] Kaiser, M., "A tutorial in connectome analysis: topological and spatial features of brain networks," *Neuroimage* 57 (3), 892-907 (2011).
- [13] Coleman, T. F. and More, J. J., "Estimation of Sparse Jacobian Matrices and Graph Coloring Problems," *SIAM Journal on Numerical Analysis* 20 (1), 187-209 (1983).
- [14] Gruslys, A., Sawiak, S. and Ansoerge, R., "3000 non-rigid medical image registrations overnight on a single PC," In Nuclear Science Symposium and Medical Imaging Conference IEEE, 3073-3080 (2011).
- [15] Supekar, K., Menon, V., Rubin, D., Musen, M. and Greicius, M. D., "Network analysis of intrinsic functional brain connectivity in Alzheimer's disease," *PLoS computational biology* 4 (6), e1000100 (2008).